Journal of Physics: Conference Series **633** (2015) 012028 doi:10.1088/1742-6596/633/1/012028

A novel method for determining the mean-field directly from the single particle matter density

S. Shlomo[1,2], M. R. Anders[1] and I. Talmi[2]
1Cyclotron Institute, Texas A&M University, College Station, Texas 77840
2The Weizmann Institute of Science, Rehovot, Israel

E-mail: s-shlomo@tamu.edu; manders14@tamu.edu; igal.talmi@weizmann.ac.il

Abstract. We present a novel method, using the single particle Schrodinger equation, to determine the central potential directly from the single particle matter density and its first and second derivatives. As an example, we consider the experimental data for the charge density difference between the isotones ^{206}Pb – ^{205}Tl that corresponds to the shell model $3s_{1/2}$ proton orbit, and determine the corresponding single particle potential (mean-field). We also present results of least-square fits to parametrized single particle potentials.

1. Introduction

The shell model, which is based on the assumption that nucleons in the atomic nucleus move independently in single particle orbits associated with a single particle potential, has been very successful in explaining many features of nuclei [1]. In this work we present a novel method, using the single particle Schrodinger equation for a wave function $\Psi(\vec{r})$ with eigenenergy E, to determine the central potential $V(\vec{r})$ directly from the measured single particle matter density, $\rho(\vec{r}) = [\Psi(\vec{r})]^2$ and its first and second derivatives, assuming known for all $\vec{r}$. We apply the method to the experimental data of the charge distribution of the proton $3s_{1/2}$ orbit given by the charge density difference, $\Delta\rho_c(r)$, between charge density distributions of the isotones ^{206}Pb – ^{205}Tl, determined by analysis of elastic electron scattering measurements [2].

We point out that the resulting single particle potential, if found, will provides a stringent limit on the effects of short correlation on the expected values of long-range operators, an important test for the shell model. The potential can also be used as an additional experimental constraint in determining a modern energy density functional (EDF) for more reliable prediction of properties of nuclei and nuclear matter [3,4]. In the next section we present the novel method and in section III we present some results with the conclusion given in section IV. Some results were presented in Ref. [5].

2. Formalism

Consider the single particle Schrodinger equation,

$$-\frac{\hbar^2}{2m}\Delta\Psi + V\Psi = E\Psi \,, \tag{1}$$

where $V(\vec{r})$ is a real local and non-singular potential and $\Delta = \vec{\nabla}\cdot\vec{\nabla}$, with $\vec{\nabla}$ being the gradient operator. Given a single particle wave function $\Psi(\vec{r})$, known for all $(\vec{r})$, with an eigenvalue E, the corresponding single particle potential V in (1) is uniquely determined [1] from

$$V(\vec{r}) = E + \frac{\hbar^2}{2m}S(\vec{r}) \,, \qquad S(\vec{r}) = \frac{\Delta\Psi(\vec{r})}{\Psi(\vec{r})} \,. \tag{2}$$

Content from this work may be used under the terms of the Creative Commons Attribution 3.0 licence. Any further distribution of this work must maintain attribution to the author(s) and the title of the work, journal citation and DOI.
Published under licence by IOP Publishing Ltd

For a nonsingular V, $\Delta\Psi(\vec{r}) = 0$ when $\Psi(\vec{r}) = 0$. Operating with Δ on $[\Psi(\vec{r})]^b$, where b is positive and real, and using the relation $\vec{\nabla}\Psi^b = b\Psi^{b-1}\vec{\nabla}\Psi$ with the definition $S(\vec{r}) = \frac{\Delta\Psi(\vec{r})}{\Psi(\vec{r})}$ of Eq. (2), we obtain the general relation

$$S(\vec{r}) = \frac{\Delta\,[\Psi(\vec{r})]^b}{b\,[\Psi(\vec{r})]^b} - \frac{b-1}{b^2}\left[\frac{\vec{\nabla}\,[\Psi(\vec{r})]^b}{[\Psi(\vec{r})]^b}\right]^2 . \tag{3}$$

Note that Eq. (2) is a special case of Eq. (3) for b=1. For b > 2, $\vec{\nabla}[\Psi(\vec{r})]^b = 0$ and $\Delta[\Psi(\vec{r})]^b = 0$ when $[\Psi(\vec{r})]^b = 0$.

In the spherical case we have for the wave function of a nucleon

$$\Psi_{nlj}(\vec{r}) = \frac{R_{nlj}(r)}{r} Y_{lj} , \tag{4}$$

where $R_{nlj}(r)$ is the radial wave function for the orbit with principle number n, orbital angular momentum l and total angular momentum j and Y_{lj} is the known spin harmonic wave function.
Using Eqs. (2) and (4) we have that nuclear central potential is given by,

$$V_{cen}(r) = E + \frac{\hbar^2}{2m}S(r) - \frac{\hbar^2}{2m}\frac{l(l+1)}{r^2} - \frac{1}{2}(1-\tau_z)V^{coul}(r) - c_{ls}\,V_{s.o.}(r) , \tag{5}$$

$$S(r) = \frac{d^2R_{nlj}}{dr^2}\frac{1}{R_{nlj}(r)} .$$

The last three terms in (5) are the centrifugal, Coulomb and spin-orbit potentials. The single particle radial density $\rho_{nlj}(r)$ is related to the square of the single particle radial wave function R^2_{nlj} by

$$R^2_{nlj}(r) = 4\pi r^2\rho_{nlj}(r) . \tag{6}$$

Adopting Eq. (1) for the radial wave-function $R_{nlj}(r)$ one can determine the central potential using Eq. (2). But this leads to numerical complication, particularly in the vicinity of the nodes of the wave function. From Eq. (1) for the radial wave-function $R_{nlj}(r)$ and Eq. (3) for b = 2 we have that the corresponding single particle potential V can be obtained from (5) by using the simple relation

$$S(r) = \frac{1}{2R^2_{nlj}}\left[\frac{d^2(R^2_{nlj})}{dr^2} - \frac{1}{2}\frac{1}{R^2_{nlj}}\left[\frac{d(R^2_{nlj})}{dr}\right]^2\right]. \tag{7}$$

From Eqs. (6) and (7) we find the relation

$$S(r) = \frac{1}{2\rho_{nlj}}\left[\frac{d^2\rho_{nlj}}{dr^2} + \frac{2}{r}\frac{d\rho_{nlj}}{dr} - \frac{1}{2\rho_{nlj}}\left(\frac{d\rho_{nlj}}{dr}\right)^2\right]. \tag{8}$$

Eqs. (8) can also be derived from Eq. (3) with b = 2 using the (real) three-dimensional wave function and the operators Δ and $\vec{\nabla}$ in spherical coordinates.
We note that for the central nuclear potential it is common to use the Woods Saxon (WS) form,

$$V(r) = V_0/[1 + exp((r - R_1)/\mathrm{a}_0)] , \tag{9}$$

where, V_0, R_1 and a_0 are the depth, half radius and diffuseness parameters, respectively. Furthermore, for the Coulomb potential we adopt the form,

$$V^{coul}(r) = Ze^2\begin{cases}(3 - r^2/R^2_{ch})/2R_{ch} & r < R_{ch}\\ 1/r & r > R_{ch}\end{cases} , \tag{10}$$

In Eqs. (10) R_{ch} is the equivalent uniform charge distribution radius, obtained from the charge root-mean-square radius, $\langle r^2\rangle_{ch}$, by

$$R^2_{ch} = (5/3)\langle r^2\rangle_{ch} . \tag{11}$$

In elastic electron-nucleus scattering measurements the charge density distribution, $\rho_c(\vec{r})$, is determined by carrying out a phase shift analysis of the cross section [6]. In theoretical models the point proton density distribution, $\rho_p(\vec{r})$ is calculated. They are related by the convolution relation

$$\rho_c(\vec{r}) = \int \rho_p(\vec{r'})\,\rho_{pfs}(\vec{r} - \vec{r'})d^3\vec{r'} , \tag{12}$$

where $\rho_{pfs}(\vec{r})$ is the charge density distribution of the free proton, commonly parametrized as

$$\rho_{pfs}(\vec{r}) = \frac{1}{8\pi a^3}e^{-r/a} , \tag{13}$$

where $a^2 = \frac{1}{12} r_{pfs}^2$ with $r_{pfs} = 0.85$ fm being the corresponding charge root mean square (rms) radius [5]. The Fourier transform for $\rho_c(r)$, Eq. (12), is given by

$$F_c(q) = F_{pfs}(q) F_p(q) \,, \tag{14}$$

where $F_c(q)$, $F_{pfs}(q)$ and $F_p(q)$, are the Fourier transforms of $\rho_c(\vec{r})$, $\rho_{pfs}(\vec{r})$ and $\rho_p(\vec{r})$, respectively. Eq. (14) can be used to determine the form factor $F_p(q)$. Then $\rho_p(r)$ can be obtained from $F_p(q)$ by the inverse Fourier transform and compared with theoretical predictions.

3. Results

Starting In Figure 1a we present (solid line) the experimental data [2] for the charge density difference,

$$\Delta\rho_c(r) = \rho_c(r;\, ^{206}\mathrm{Pb}) - \rho_c(r;\, ^{205}\mathrm{Tl}), \tag{15}$$

between the isotones ^{206}Pb – ^{205}Tl. It is normalized to a total charge of one proton. The dotted lines indicate the experimental uncertainty. The two nodes associated with the proton $3s_{1/2}$ orbit are clearly seen in the figure. The experimental values of the charge rms radii of ^{206}Pb and ^{205}Tl are 5.4897 and 5.4792 fm, respectively. To assess the possible rearrangement effect (from ^{205}Tl to ^{206}Pb) on the charge rms radius of the 81 protons core in ^{206}Pb, we assume that it increases by 0.005 fm, similar to the change between nuclei in this region [7]. The rearrangement effect is approximated (see Ref. [7]) by scaling the charge distribution of ^{205}Tl . We thus obtain

$$\Delta\rho_{Rc}(r) = \rho_c(r;\, ^{206}\mathrm{Pb}) - \alpha^3 \rho_c(\alpha r;\, ^{205}\mathrm{Tl}), \tag{16}$$

where the scaling parameter α = 5.4792/(5.4792 + 0.005) = 0.9990 is the ratio between the charge rms radius of ^{205}Tl to that of the 81 core protons in ^{206}Pb. The results for $\Delta\rho_{Rc}(r)$ is shown in Figure1a (dashed line). Using the relation (6) we determined the values of $R_p^2(r) = 4\pi r^2 \Delta\rho_p(r)$ and $R_{Rp}^2(r) = 4\pi r^2 \Delta\rho_{Rp}(r)$, deduced from the results of Figure 1a using Eqs. (12) and (14), shown as solid and dashed lines in Figure 1b. The dotted lines indicate the experimental uncertainty. The magnitude of the difference between $R_p^2(r)$ and $R_{Rp}^2(r)$ is similar to that of the experimental uncertainty.

The corresponding potentials, for $R_p^2(r)$ and $R_{Rp}^2(r)$ of Figure 1b, obtained by employing Eqs. (5) and (6), are shown in Figure 2a by the solid and dashed lines, respectively. The dotted lines (constant potentials) are extracted from fits of the corresponding wave-function in the vicinity of the minima to Ψ= Asin(kr+ϕ) + C. The Coulomb potential of Eq. (10), with $R_{ch} = 7.1$ fm, was adopted in the calculations. For the $3s_{1/2}$ orbit, there is no contribution from the centrifugal and spin-orbit potentials. Note the large uncertainties in the extracted potential in the vicinity of the nodes (at 2.6 and 4.9 fm).

We have therefore considered several nuclear central potentials with parameters obtained by fits to the corresponding experimental data, taking into account the Coulomb potential, Eq. (10). In Figure 2b the resulting potentials fitted to $R_p^2(r)$ of Figure 1b. Solid and dashed lines are fits to multipole lines potential to the solid and dashed lines of Figure 1b, respectively. We obtained good agreement with data with χ^2 /N = 1.15 and 1.81, respectively. The dashed-double dotted and dashed-dotted potential are for the fitted and the conventional Wood-Saxon potential (9) with χ^2 /N = 3.28 and 8.85 respectively.

4. Conclusions

Starting from the single particle Schrodinger equation for the function $\Psi(\vec{r})$, with eigen-energy *E*, we have derived a novel method for determining the corresponding single particle potential *V* from $[\Psi(\vec{r})]^b$, where b is a real number, assuming that $[\Psi(\vec{r})]^b$, $\vec{\nabla}\Psi$ and $\Delta[\Psi(\vec{r})]^b$ are known for all positions ($\vec{r}$), see Eqs. (2) and (3). It is clear from the Schrodinger equation that for a nonsingular *V*, $\Delta\Psi(\vec{r}) = 0$ when $\Psi(\vec{r}) = 0$. For b > 2 this condition is extended to the requirements that, $\vec{\nabla}[\Psi(\vec{r})]^b = 0$ and $\Delta[\Psi(\vec{r})]^b = 0$ when $[\Psi(\vec{r})]^b = 0$. For b = 2, we have from Eqs. (2) and (3) that the potential

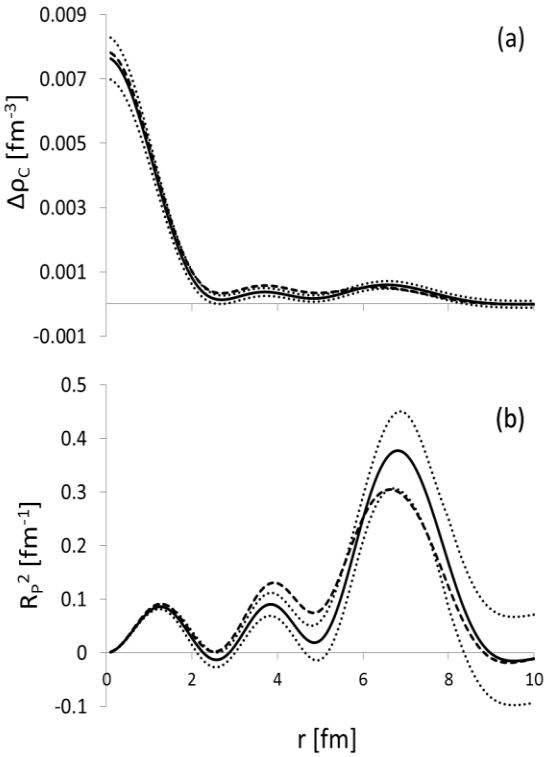


Figure 1. See text.

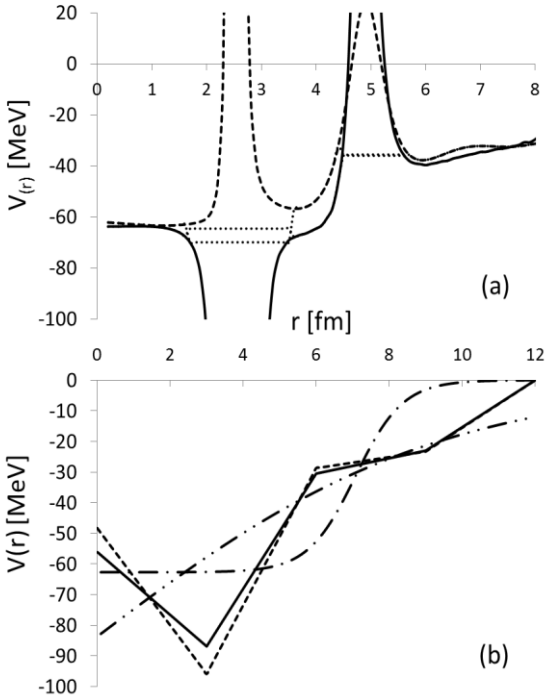


Figure 2. See text.

$V(\vec{r})$ is given in term of the corresponding single particle matter density $\rho(\vec{r})$ (for real $\Psi(\vec{r})$) and its first and second derivatives.

As an example, we considered the experimental data for the charge density difference between the isotones ^{206}Pb – ^{205}Tl that corresponds to the shell model $3s_{1/2}$ proton orbit, and determined the corresponding single particle potential (mean-field). We also presented results of least-square fits to parametrized single particle potentials. The $3s_{1/2}$ wave functions of the determined potentials reproduce fairly well the experimental data within the quoted errors. The fair agreement with fitted potentials may be an indication that effects of short range correlations on charge distributions are not significant. More accurate experimental data, with uncertainty smaller by a factor of two or more, may answer the question how well can the data be reproduced by a calculated $3s_{1/2}$ wave function.

5. References

[1] A. de Shalit and I. Talmi, *Nuclear Shell Model*, Academic Press, New York, N.Y., 1963.
[2] B. Frois, et al, Nucl. Phys. **A396**, 409c (1983).
[3] B. K. Agrawal, S. Shlomo and V. Kim Au, Phys. Rev. C **72**, 014310-1-13 (2005).
[4] S. Shlomo, in *The Universe Evolution: Astrophysical and Nuclear Aspects,"* Eds., L. Blokhintsev and I. Strakovsky, Nova Science Publishers, 2013.
[5] M. R. Anders, S. Shlomo and I. Talmi, ArXiv:1504.05507 [nucl-th]; Sub. to Phys. Lett B.
[6] L. R. B. Elton, *Nuclear Sizes*, Oxford University Press, London, 1961.
[7] H. Euteneuer, J. Friedrich and N. Voegler, Nucl. Phys. **A298**, 452 (1978).

Acknowledgments

S. S. thanks The Weizmann Institute of Science for the kind hospitality. This work was supported in part by US Department of Energy under Grant No. DOE-FG03-93ER40773.